

FULL ARTICLE

## Oxygen-dependent delayed fluorescence measured in skin after topical application of 5-aminolevulinic acid

Floor A. Harms<sup>1</sup>, Wadim M. I. de Boon<sup>1</sup>, Gianmarco M. Balestra<sup>1,2</sup>, Sander I. A. Bodmer<sup>1</sup>, Tanja Johannes<sup>1</sup>, Robert J. Stolker<sup>1</sup>, and Egbert G. Mik<sup>\*,1</sup>

<sup>1</sup> Department of Anesthesiology, Laboratory of Experimental Anesthesiology, ErasmusMC, University Medical Center Rotterdam, Rotterdam, The Netherlands

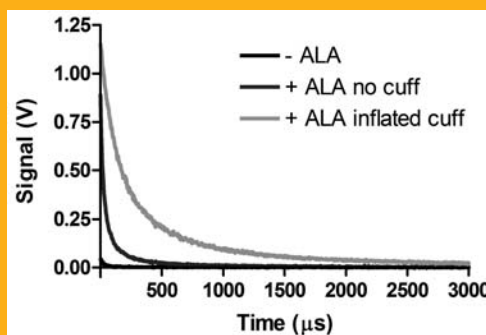
<sup>2</sup> Department of Intensive Care, University Hospital Basel, Basel, Switzerland

Received 13 May 2011, revised 26 June 2011, accepted 27 June 2011

Published online 20 July 2011

**Key words:** oxygen-dependent quenching, luminescence, tissue oxygen, mitochondrial oxygen, protoporphyrin IX, PpIX

Mitochondrial oxygen tension can be measured in vivo by means of oxygen-dependent quenching of delayed fluorescence of protoporphyrin IX (PpIX). Here we demonstrate that delayed fluorescence is readily observed from skin in rat and man after topical application of the PpIX precursor 5-aminolevulinic acid (ALA). Delayed fluorescence lifetimes respond to changes in inspired oxygen fraction and blood supply. The signals contain lifetime distributions and the fitting of rectangular distributions to the data appears more adequate than mono-exponential fitting. The use of topically applied ALA for delayed fluorescence lifetime measurements might pave the way for clinical use of this technique.



Oxygen-dependent delayed fluorescence measured on the forearm of a volunteer before and after inflation of a blood pressure cuff.

### 1. Introduction

The adequate supply of oxygen by inhalation and subsequent transport to tissues via the circulating blood is a *conditio sine qua non* for mammalian cells to sustain life. Molecular oxygen is the primary oxidant in biological systems and its ultimate destination in vivo is the mitochondria where it is used in oxidative phosphorylation [1]. Besides being indispensable for the energy production of our cells, oxygen is known to play a role in many other biochem-

ical processes and mammalian tissue contains a large number of oxygen consuming enzymes [2].

Many techniques have been developed for measuring oxygen in vivo [3], because of the importance of adequate oxygen supply. However, due to invasiveness or the need of injection of foreign compounds into the circulation, most techniques have been restricted to preclinical use in laboratory animals. An excellent example of this is the phosphorescence quenching technique, originally developed by Vanderkooi and Wilson in the late 1980s [4].

\* Corresponding author: e-mail: e.mik@erasmusmc.nl, Phone: +31 10 7043310, Fax: +31 10 7044725

Oxygen-dependent quenching of phosphorescence of metallo-porphyrin-based dyes relies on the injection of the dye in experimental animals. This allows for the measurement of oxygen tension ( $PO_2$ ) in the microcirculation [5, 6] or interstitium [7, 8], depending on the site of injection. The oxygen tension ( $PO_2$ ) can be calculated from the phosphorescence decay kinetics. Once calibrated, phosphorescence lifetime measurements do not require recalibration [9]. Furthermore, because the technique measures lifetimes, and not intensities, it is insensitive to changes in tissue optical properties. Despite these favorable properties, the need for injection of potentially toxic oxygen-sensitive dyes has prevented its clinical use till today.

In order to circumvent this drawback we researched the possibilities to use endogenous porphyrin for measuring oxygen. Recently we demonstrated that the optical properties of endogenous protoporphyrin IX (PpIX) enables quantitative oxygen measurements by means of oxygen-dependent quenching of delayed fluorescence [10]. 5-Aminolevulinic acid (ALA) enhanced PpIX is synthesized inside the mitochondria [11] and can act as mitochondrially located oxygen-sensitive dye. We successfully measured mitochondrial  $PO_2$  (mito $PO_2$ ) in cultured cells [10], rat liver [12] and rat heart [13].

ALA is a precursor in porphyrin synthesis and its application induces the accumulation of PpIX inside mitochondria [14]. ALA is clinically used in photodynamic diagnosis and therapy of cancer [15–17]. Besides systemic application by oral intake or intravenous injection, ALA can be topically applied to tissue in order to enhance PpIX levels locally [18, 19]. If the latter approach would prove to be feasible for delayed fluorescence measurements this could pave the way for exploring its clinical applications.

In this study we tested the feasibility of measuring oxygen-dependent delayed fluorescence in skin after topical application of ALA. To this end, 2.5% ALA cream was topically applied for 3 hours on the skin of anesthetized and mechanically ventilated rats. Delayed fluorescence was detected from the side of application and the oxygen-dependency of the lifetime was tested by various measures. Three different methods to analyze the delayed fluorescence signals were compared. We also performed a pilot experiment on the forearm of a healthy volunteer.

## 2. Materials and methods

### 2.1 Principle of measurement

The background of the PpIX delayed fluorescence technology is described in detail elsewhere [10, 12]. In short, PpIX is the final precursor of heme in

the heme biosynthetic pathway (Figure 1 upper panel). PpIX is synthesized in the mitochondria, and administration of ALA substantially enhances the PpIX concentration. Since the conversion of PpIX to heme is a rate-limiting step, administration of ALA causes accumulation of PpIX inside the mitochondria. PpIX possesses a triplet state ( $T_1$ ) that reacts strongly with oxygen, making the  $T_1$  lifetime oxygen-dependent (Figure 1 lower panel). Population of  $T_1$  occurs upon photo-excitation with a pulse of light, and bidirectional intersystem crossing causes the emission of red delayed fluorescence. The lifetime of the delayed fluorescence reflects the  $T_1$  lifetime and is therefore also oxygen-dependent.

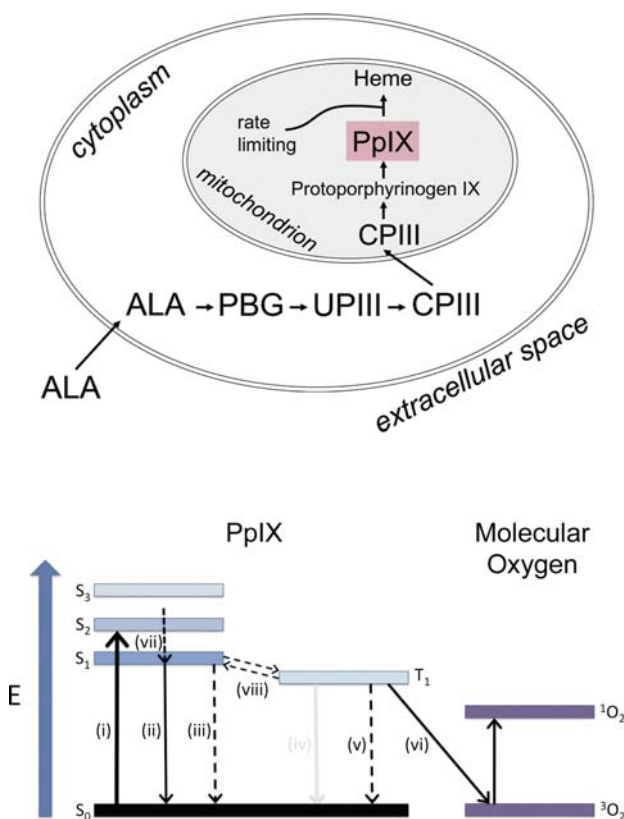


**Figure 1** (online color at: [www.biophotonics-journal.org](http://www.biophotonics-journal.org)) Principle by which ALA administration enhances mitochondrial PpIX levels (upper panel) and the Jablonski diagram of states and state transitions of PpIX and its interaction with oxygen (lower panel). ALA, 5-aminolevulinic acid; PBG, porphobilinogen; UPIII, uroporphyrinogen III; CPIII, coproporphyrinogen III; and PpIX, protoporphyrin IX.  $S_0$ ,  $S_1$ ,  $S_2$  and  $S_3$  represent the ground state and first, second and third excited singlet states, respectively.  $T_1$  represent the first excited triplet states of PpIX and  $^3O_2$  and  $^1O_2$  are the triplet ground state and excited singlet state of oxygen. Absorption (i), fluorescence and delayed fluorescence (ii), radiationless transitions (iii and v), phosphorescence (iv), energy transfer (vi), internal conversion (vii) and bi-directional intersystemcrossing (viii).

## 2.2 Lifetime analysis

When excited by a light pulse, the delayed fluorescence (~610–740 nm) intensity decreases at a rate dependent on the surrounding oxygen pressure. The relationship between the measured decay time and the PO<sub>2</sub> is given by the Stern-Volmer equation:

$$PO_2 = \frac{\frac{1}{\tau} - \frac{1}{\tau_0}}{k_q} \quad (1)$$

where  $\tau$  is the measured decay time,  $\tau_0$  is the decay time at an oxygen pressure of zero and  $k_q$  is the quenching constant. Although the calibration constants have been determined in rat liver [12] and rat heart [13],  $\tau_0$  and  $k_q$  are not validated for our current application in skin. Especially the temperature dependency of  $\tau_0$  and  $k_q$  remain to be determined. Therefore, instead of providing quantitative PO<sub>2</sub> values we restrict ourselves to reporting our data in terms of reciprocal lifetimes ( $R_\tau$ ):

$$R_\tau = \frac{1}{\tau} = k_q PO_2 + \frac{1}{\tau_0} \quad (2)$$

Equations (1) and (2) describe the relationship between the PO<sub>2</sub> and the phosphorescence lifetime in case of a homogeneous oxygen distribution. However, large nonuniformities in oxygen pressure exist in vivo, resulting in a phosphorescence signal that in general can be described by an integral over an exponential kernel:

$$y(t) = \int_0^t \exp(-\lambda t) f(\lambda) d\lambda \quad (3)$$

where  $f(\lambda)$  denotes the spectrum of reciprocal lifetimes that should be determined from the finite data set  $y(t)$ . The Exponential Series Method (ESM) has been proven reliable and robust [12, 20] for retrieving information about the spectrum  $f(\lambda)$  in the case of delayed luminescence lifetime measurements. According to ESM the reciprocal lifetime distribution can be retrieved from the data by finding the weight factors of a finite set of discrete reciprocal lifetimes:

$$Y(t) = \sum w_i \exp(-R_{\tau_i} t) \quad (4)$$

where  $Y^*(t)$  are the normalized phosphorescence data and  $w_i$  is the weight factor for the according reciprocal lifetime  $R_{\tau_i}$  ( $w_i = 0$  and  $\sum w_i = 1$ ). For analysis of our data we used a set of 15 equally distributed  $R_{\tau_i}$ 's in the range 0.005 to 0.122  $\mu\text{s}^{-1}$ , corresponding to a broad lifetime range from 8 till 200  $\mu\text{s}$ . The average value of  $R_\tau$ , denoted by  $\langle R_\tau \rangle$ , can be retrieved from the distribution by:

$$\langle R_\tau \rangle = \sum w_i R_{\tau_i} \quad (5)$$

Besides the ESM method, we used Mono-Exponential Analysis (MEA) and the approach published by Golub et al. [21] in which the heterogeneity in oxygen pressure is analyzed by fitting distributions of quencher concentration to the delayed luminescence data. Corresponding to their work, the fitting function for a simple rectangular distribution with a mean PO<sub>2</sub>  $Q_m$  and a PO<sub>2</sub> range from  $Q_m - \delta$  till  $Q_m + \delta$  is

$$Y_R(t) = \exp[-(k_0 + k_q Q_m) t] \cdot \sinh(k_q \delta t) / k_q \delta t \quad (6)$$

where  $Y_R(t)$  is the normalized phosphorescence data,  $k_0$  is the first-order rate constant for phosphorescent decay in the absence of quencher, and  $\delta$  is half the width of the rectangular distribution. For the case of unknown calibration constants Eq. (5) can be rewritten as:

$$Y_R(t) = \exp[-R_\tau t] \cdot \sinh(\Delta t) / \Delta t \quad (7)$$

where  $\Delta$  is a measure of the heterogeneity in reciprocal lifetime  $R_\tau$ . We refer to this approach as the Rectangular Distribution Method (RDM).

## 2.3 Experimental setup

The excitation source was an Opolette 355-I (Opo-tek, Carlsbad, CA, USA), a compact computer-controlled tunable laser providing pulses with a specified duration of 4–10 ns and typically 2–4 mJ/pulse over the tunable range of 410 to 670 nm. The laser was coupled into a Fiber Delivery System (Opo-tek, Carlsbad, CA, USA) consisting of 50 mm plano-convex lens, X–Y fibermount and a 2 meter fiber with a core diameter of 1000  $\mu\text{m}$ . This fiber was coupled to a custom made reflection probe by an In-Line Fiber Optic Attenuator (FOA-Inline, Avantes b.v., Eerbeek, The Netherlands). The reflection probe consisted of two 1000  $\mu\text{m}$  fibers with a length of 2 meters (P1000-2-VIS-NIR, Ocean Optics, Dunedin, FL, USA) mounted at the common end into a stainless steel holder with a separation of 1 mm between the fibers. The light output of the excitation branch was set at 200  $\mu\text{J}$ /pulse as measured by a FieldMate laser power meter with PowerMax PS19 measuring head (Coherent Inc., Santa Clara, CA, USA). Measurements were performed with the reflection probe at 5 mm from the skin. Due to an output angle of 25.4° this resulted in an illuminated spot with a diameter of approximately 3.3 mm. Corresponding fluencies were 2.4 mJ/cm<sup>2</sup> per pulse and 0.15 J/cm<sup>2</sup> per measurement.

The PpIX signal was detected by a gated microchannel plate photomultiplier tube (MCP-PMT R5916U series, Hamamatsu Photonics, Hamamatsu, Japan). The MCP-PMT was custom adapted with an

enhanced red-sensitive photocathode having a quantum efficiency of 24% at 650 nm. The MCP-PMT was mounted on a gated socket assembly (E3059-501, Hamamatsu Photonics, Hamamatsu, Japan) and cooled to  $-30\text{ }^{\circ}\text{C}$  by a thermoelectric cooler (C10373, Hamamatsu Photonics, Hamamatsu, Japan). The MCP-PMT was operated at a voltage in the range of 2300 V–3000 V by a regulated high-voltage DC power supply (C4848-02, Hamamatsu Photonics, Hamamatsu, Japan). The detection fiber was fit into an Oriol Fiber Bundle Focusing Assembly (Model 77799, Newport, Irvine, CA, USA) which was coupled to the MCP-PMT by an in-house built optics consisting of a filter-holder, a plano convex lens (BK-7, Opto-Sigma, Santa Ana, CA, USA) with focal length of 90 mm and an electronic shutter (04 UTS 203, Melles Griot, Albuquerque, NM, USA). The shutter was controlled by an OEM Shutter Controller Board (59 OSC 205, Melles Griot, Albuquerque, NM, USA) and served as protection for the PMT, which was configured for the “normally on” mode. The PpIX emission light was filtered by a combination of a 590 nm longpass filter (OG590, Newport, Irvine, CA, USA) and a broadband (600–750 nm) bandpassfilter (Omega Optical, Brattleboro, VT, USA).

The output current of the photomultiplier was voltage-converted by an in-house built amplifier with an input impedance of 440 ohm, 400 times voltage amplification and a bandwidth around 20 Mhz. Data-acquisition was performed by a PC-based data-acquisition system containing a 10 MS/s simultaneous sampling data-acquisition board (NI-PCI-6115, National Instruments, Austin, TX). The amplifier was coupled to the DAQ-board by a BNC interface (BNC-2090A, National Instruments, Austin, TX). The data-acquisition ran at a rate of 10 mega samples per second and 64 laser pulses (repetition rate 20 Hz) were averaged prior to analysis. Control of the setup and analysis of the data was performed with software written in LabView (Version 8.6, National Instruments, Austin, TX, USA).

## 2.4 Experimental procedures

The protocol was approved by the Animal Research Committee of the ErasmusMC University Medical Center Rotterdam. Animal care and handling were performed in accordance with the guidelines for Institutional and Animal Care and Use Committees.

A total of 6 male Wistar rats (Charles River, Wilmington, MA, USA, body weight  $292 \pm 25,5\text{ g}$ ) were used in this study. The animals were anesthetized by an intraperitoneal injection of a mixture of ketamine  $90\text{ mg kg}^{-1}$  (Alfasan, Woerden, The Netherlands), medetomidine  $0.5\text{ mg kg}^{-1}$  (Sedator Eurovet Animal Health BV, Bladel, The Netherlands), and atropine

$0.05\text{ mg kg}^{-1}$  (Centrofarm Services BV, Etten-Leur, The Netherlands). Mechanical ventilation was performed via tracheotomy. Ventilation was adjusted on end-tidal  $\text{PCO}_2$ , keeping the arterial  $\text{PCO}_2$  between 35 and 40 mmHg. Variations in  $\text{FiO}_2$ , the fraction of inspired oxygen, were made by mixtures of oxygen and nitrogen.

A polyethylene catheter (outer diameter 0.9 mm) was inserted into the right jugular vein for the intravenous administration of fluids. Arterial blood pressure and heart rate were monitored with a similar catheter in the right carotid artery. Ketamine ( $50\text{ mg kg}^{-1}\text{ h}^{-1}$ ) and crystalloid solution (Ringer lactate,  $5\text{ mL kg}^{-1}\text{ h}^{-1}$ ) were infused intravenously for maintaining anaesthesia and fluid balance. Body temperature was rectally measured and kept at  $38^{\circ}\text{C} \pm 0.5\text{ }^{\circ}\text{C}$  by means of a heating pad.

PpIX was induced by topical application of 2.5% ALA cream. A mixture of hydrophilic cremor lanette (Lanettecrème I FNA, Bipharma, Weesp, The Netherlands) and 2.5% 5-aminolevulinic acid (Sigma-Aldrich, St. Louis, MO, USA) was made just before use and administered topically on the abdominal skin after hair removal. The latter was accomplished by shaving and hair removal cream (Veet, Reckitt Benckiser Co., Slough, UK). The exposed skin was covered with an adhesive film and, to prevent premature exposure of PpIX to light, the area was covered with aluminium foil. The delayed fluorescence lifetime measurements were started three hours after the application of ALA cream. First the baseline delayed fluorescence was measured at an  $\text{FiO}_2$  of 0.4 and subsequently, after a stabilisation period of 5 minutes, measurements were performed during 1.0  $\text{FiO}_2$  ventilation. The experiment was terminated by euthanasia of the animal using an overdose of Euthasol (ST Farma, Raamsdonksveer, The Netherlands).

The experiment in human skin was voluntarily performed on the forearm of the principal investigator (E.G.M.). A small aliquot of 2.5% ALA-cream was topically applied under adhesive foil and protection from light for 3 hours. Delayed fluorescence was measured under normal conditions and 2 minutes after cessation of blood flow by inflation of a blood-pressure cuff around the arm.

## 3. Results

Topical application of ALA to the abdominal skin of rats induced detectable delayed fluorescence signal. Figure 2 shows the signals observed in a rat from areas of the skin with and without direct ALA exposure. The area on which ALA was topically applied shows a clear signal. This is in contrast to the area without ALA in which the signal is very faint. The

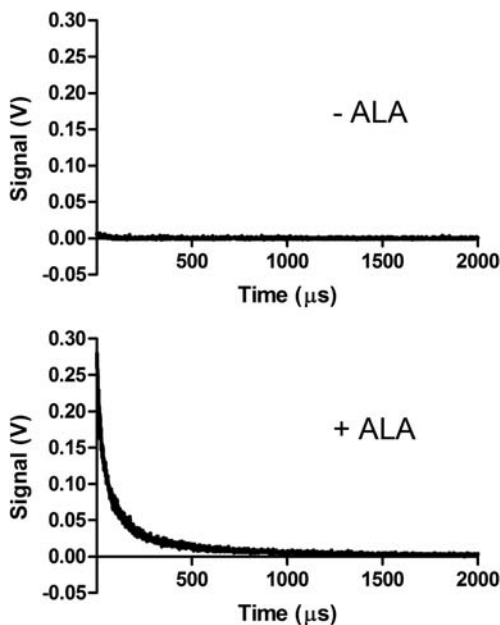


**Figure 2** Examples of signals obtained from areas of skin on the abdomen of a rat not exposed (upper panel) and exposed to topically administered ALA for 3 hours.

latter was most probably due to some systemic ALA uptake and distribution. No signal was detectable in skin from rats not exposed to ALA.

The oxygen-dependency of the delayed fluorescence is demonstrated in Figure 3. A change in inspired oxygen fraction from 0.4 (40% oxygen in the ventilation gas) to 1.0 (breathing with 100% oxygen) resulted in a faster decay of the delayed fluorescence signal, corresponding to higher oxygen levels in the skin tissue. Conversely, cessation of microvascular blood flow by applying pressure to the skin with the detection probe resulted in a slower decay. This is in accordance with decreased oxygen levels in the skin tissue due to oxygen consumption under blocked oxygen supply.

Analysis of the delayed fluorescence by means of the ESM method reveals that the delayed fluorescence signal is not simply mono-exponential, as would be the case if oxygen would be homogeneously distributed in the skin. The distribution of reciprocal lifetimes shows a much more complex pattern of which examples are shown in Figure 4. The ESM analysis generally shows a left-skewed distribution (i.e. towards short reciprocal lifetimes corresponding to low oxygen levels) with a considerable part of the signal arising from areas emitting long lived delayed fluorescence. Upon increasing the  $FiO_2$  from 0.4 to 1.0 the distribution moves towards the right and the fraction of the shortest reciprocal lifetime decreases. Both phenomena correspond to an increase in oxygen levels in the skin.

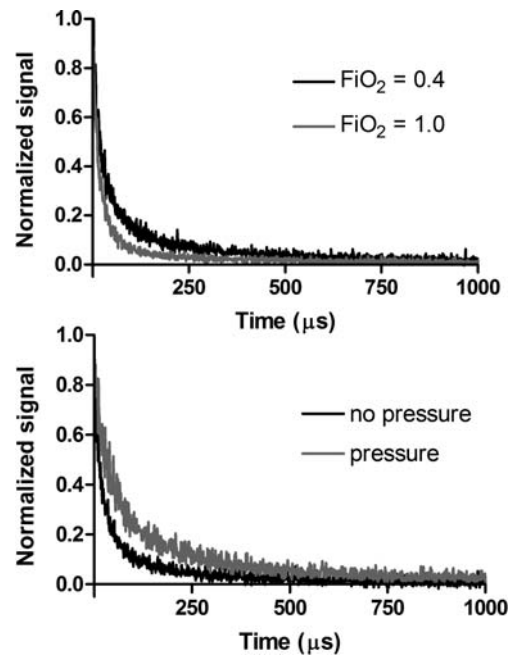


**Figure 3** Normalized delayed fluorescence traces measured in abdominal skin of rats after 3 hours exposure to topically administered ALA. Increasing  $FiO_2$  from 0.4 to 1.0 results in faster decay of delayed fluorescence (upper panel). Application of pressure on the skin by the measurement probe results in a slower decay of delayed fluorescence (lower panel).

Although the exponential series method (ESM) has been proven to be reliable and robust for delayed fluorescence measurements, the calculations are relatively time consuming (seconds to tens of seconds) and in its current form too slow for real-time implementation under non-steady state circumstances. Therefore we compared the average lifetimes retrieved by both mono-exponential analysis (MEA) and the rectangular distribution method (RDM) to the ESM. Figure 5 shows the effects of increasing  $FiO_2$  in 6 rats on the average reciprocal lifetime  $\langle R_\tau \rangle$  as found with the ESM. 5 out of 6 rats respond to an increase in  $FiO_2$  with the expected increase in  $\langle R_\tau \rangle$ . The lower two panels show that in general MEA has the tendency to overestimate the average delayed fluorescence lifetime. The average lifetimes obtained by RDM are in good agreement with the ESM.

To test whether topical application of ALA also induces measurable oxygen-dependent delayed fluorescence in hairless human skin we conducted a pilot experiment on inside of the forearm of the principal investigator. Figure 6 shows that delayed fluorescence is readily measured after 3 hours of topical application of ALA. Also, cessation of blood flow to the limb by inflating a cuff around the arm leads to slower decay kinetics of the delayed fluorescence signal.

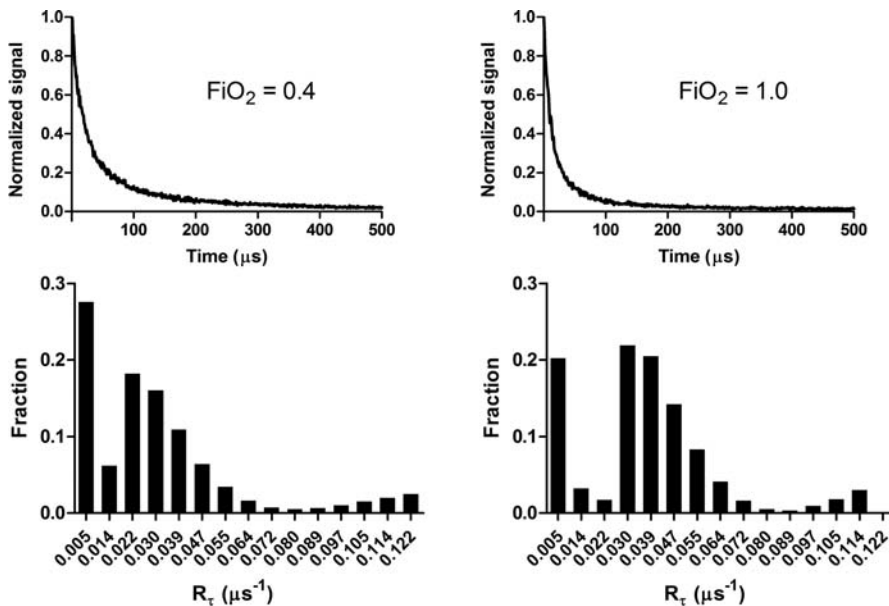


**Figure 4** Examples of delayed fluorescence signals at different  $\text{FiO}_2$  (upper panel) and the corresponding distributions of reciprocal lifetimes as obtained by ESM (lower panel).

#### 4. Discussion and conclusion

In this work, we present a method to induce and measure oxygen-dependent delayed fluorescence in skin. The clear advantage of topical application of ALA over systemic administration is the reduction of potential side effects. The measurement equipment is fiber-based and robust and can be adapted for clinical use. We demonstrate that 3 hours after topical application of a low-dose ALA crème (2.5%), oxygen-dependent delayed fluorescence is easily observed from abdominal skin in rats and also human skin on the forearm. The delayed fluorescence signal contained a complex (reciprocal) lifetime distribution as determined with ESM. While MEA had the tendency to overestimate the average lifetime, RDM provided results that were comparable to ESM analysis.

Although ALA is systemically administered to patients in the setting of photodynamic therapy and diagnosis [14–16] without significant side effects, the photosensitization of the entire skin and retina asks for special precautions. The topical application of ALA derivatives has become a widely used method in photodynamic therapy of non-melanoma skin cancers [22]. Since concerns about photosensitization are limited to the exposed skin area, which can easily be protected from light, patients remain ambulant and are often treated in an out-of-hospital setting. Furthermore, the safety of this approach has led to the use of photodynamic therapy on benign skin lesions, like acne [23] and hidradenitis [24]. Therefore, our finding that topical application of a relatively low dose of ALA crème induces measurable levels of oxygen-dependent delayed fluorescence might prove an important step in bringing this

technique to applications in human beings. However, repeated delayed fluorescence measurements could exceed the light doses used for photodynamic therapy. Therefore, for clinical use one should strive to minimize excitation light levels.

In its calibrated form, the technique of oxygen-dependent quenching of delayed fluorescence of PpIX allows for the measurement of mitochondrial oxygen tension in living cells [10] and ex vivo and in vivo tissues [12, 13]. For its application in skin, the calibration constants remain to be determined, but the oxygen-dependence of the signal was evident in the present study from analysis of the reciprocal lifetime distributions. The reciprocal lifetimes are linearly dependent on the oxygen levels and this makes the technique useful even in the absence of true calibration. For example, dynamic measurement of the reciprocal lifetimes during photodynamic therapy can give insight in the rate of oxygen disappearance due to oxygen-radical formation. This could be helpful for optimizing the effect of treatment [25, 26].

The ESM in its current form is too slow for real-time analysis of delayed fluorescence signals and therefore we applied two other methods for lifetime analysis, mono-exponential analysis (MEA) and the rectangular distribution method (RDM). As in the case of phosphorescence lifetime measurements, the MEA overestimates the average lifetime [27]. Although the underlying distributions are more complex than a simple rectangular distribution, the RDM provided average lifetimes comparable to those obtained by ESM.

Overall, our study shows that implementation of the technique of oxygen-dependent quenching of delayed fluorescence is feasible in skin using topical application of ALA crème. The delayed fluorescence

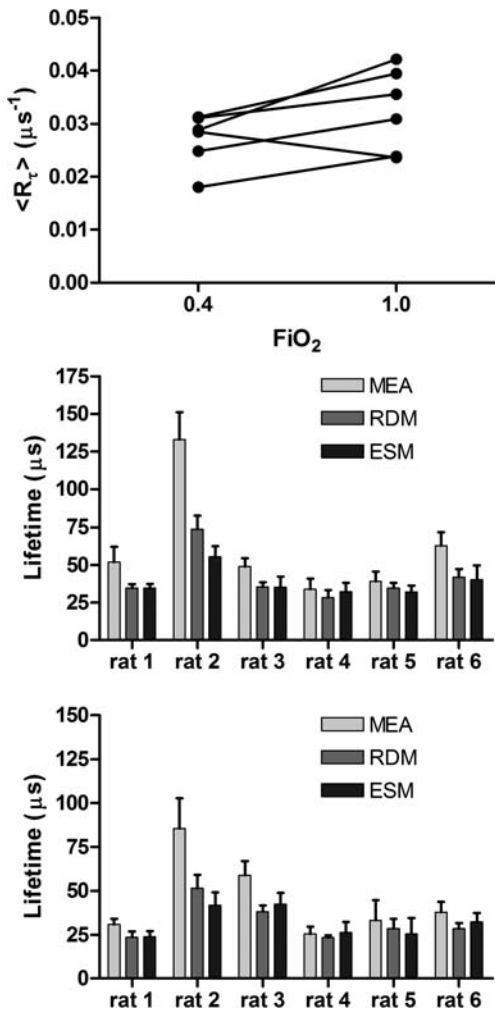


**Figure 5** Effect of the increase in  $\text{FiO}_2$  from 0.4 to 1.0 on the average reciprocal lifetime  $\langle R_t \rangle$  as obtained with ESM (upper panel). Average lifetime obtained by mono-exponential analysis (MEA), rectangular distribution method (RDM) and exponential series method (ESM) at  $\text{FiO}_2 = 0.4$  (middle panel) and at  $\text{FiO}_2 = 1.0$  (lower panel).

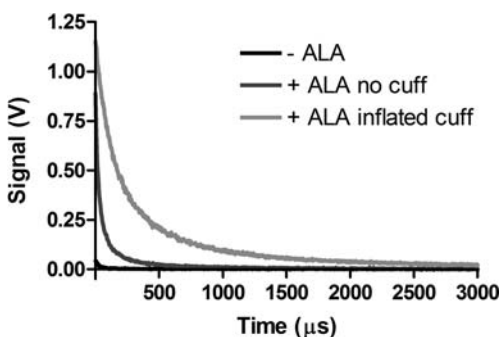


**Figure 6** Measurement of delayed fluorescence on the forearm of a volunteer. Topical ALA administration induced a delayed fluorescence signal of which the lifetime increased upon inflation of a blood pressure cuff around the arm.

signals contain complex lifetime distributions and the lifetime analysis has to be adapted accordingly. The RDM is a fast and easy to implement alternative to the ESM if one needs real-time analysis in non-steady state situations. Clinical applications of the technique might range from measuring oxygen during photodynamic therapy to monitoring cellular oxygen availability in the skin of critically ill patients.

**Acknowledgements** This work is financially supported by a Life Sciences Pre-Seed Grant (grant no 40-41300-98-9037) from the Netherlands Organization for Health Research and Development (ZonMW) and, in part, by the Young Investigator Grant 2009 (awarded to E.G.M.) from the Dutch Society of Anesthesiology.

**Conflict of Interest** E.G.M is founder and shareholder of Photonics Healthcare B.V., a company aimed at making the delayed fluorescence lifetime technology available to a broad public. Photonics Healthcare B.V. holds the exclusive licenses to several patents regarding this technology, filed and owned by the Academic Medical Center in Amsterdam and the Erasmus Medical Center in Rotterdam, The Netherlands.



**Floor A. Harms** is a medical doctor and Ph.D. student at the Department of Anesthesiology at the Erasmus MC – University Medical Center, Rotterdam. Her work focuses on mitochondrial oxygenation in sepsis, based on measurement of the oxygen-dependent delayed fluorescence of endogenous protoporphyrin IX.



**Wadim M. I. de Boon** is a medical student at the University of Amsterdam, The Netherlands. In 2008, he enrolled the Honours Program for which he performed research at the Department of Anesthesiology at the Erasmus MC – University Medical Center Rotterdam, The Netherlands. His current interest lies in the field of plastic and cardiothoracic surgery. At present, he performs a scientific course for his doctoral degree at the Surgical Laboratory, Department of Surgery, Academic Medical Centre, Amsterdam.



**Gianmarco M. Balestra** is an internist and intensive care medicine specialist working as a consultant in the medical intensive care unit at the University Hospital Basel, Switzerland. His scientific interest includes the pathophysiological states of the microcirculation during critical illness and in particular the myocardial oxygenation states during sepsis. He conducts his research in close collaboration with the Laboratory of Experimental Anesthesiology of the Erasmus MC in Rotterdam.



**Sander I. A. Bodmer** is a medical doctor and Ph.D. student at the Department of Anesthesiology at the Erasmus MC – University Medical Center Rotterdam, The Netherlands. His research focuses on the development and application of techniques for measuring microvascular oxygen tension based on in vivo use of phosphorescent nano-carriers.



**Tanja Johannes** is anesthesiologist and staff member at the Department of Anesthesiology at the Erasmus MC – University Medical Center Rotterdam, The Netherlands. She received her Ph.D. degree in 2011 from the University of Amsterdam. Her scientific interests include physiological and pathophysiological changes in kidney oxygenation in sepsis, studied with phosphorescence and delayed fluorescence lifetime techniques.



**Robert Jan Stolker** is professor of anesthesiology and chairman of the Department of Anesthesiology at the Erasmus MC – University Medical Center Rotterdam, The Netherlands. Besides his interests in experimental anesthesiology his scientific work covers the fields of pain medicine and resident training.



**Egbert G. Mik** is anesthesiologist-intensivist and staff member at the Departments of Anesthesiology and Intensive Care at the Erasmus MC – University Medical Center Rotterdam, The Netherlands. He received his Ph.D. degree in 2011 cum laude from the University of Amsterdam. He is heading the Laboratory of Experimental Anesthesiology and his research focuses on tissue oxygenation and oxygen metabolism in the perioperative and intensive care setting.

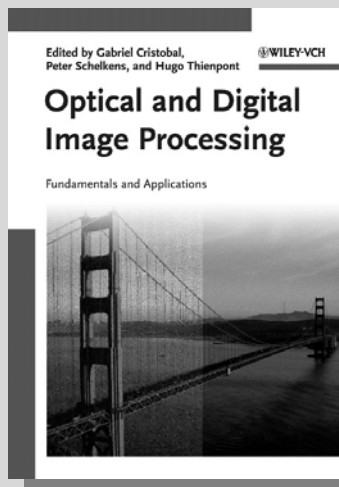
## References

- [1] P. Mitchell and J. Moyle, *Nature* **213**, 137–139 (1967).
- [2] J. M. Vanderkooi, M. Erecinska, and I. A. Silver, *Am. J. Physiol.* **260**, C1131–1150 (1991).
- [3] R. Springett and H. M. Swartz, *Antioxid. Redox. Signal.* **9**, 1295–1301 (2007).
- [4] J. M. Vanderkooi, G. Maniara, T. J. Green, and D. F. Wilson, *J. Biol. Chem.* **262**, 5476–5482 (1987).
- [5] T. Johannes, C. Ince, K. Klingel, K. E. Unertl, and E. G. Mik, *Crit. Care Med.* **37**, 1423–1432 (2009).
- [6] T. Johannes, E. G. Mik, B. Nohe, N. J. Raat, K. E. Unertl, and C. Ince, *Crit. Care* **10**, R88 (2006).
- [7] A. S. Golub, M. A. Tevald, and R. N. Pittman, *Am. J. Physiol. Heart Circ. Physiol.* **300**, H135–143 (2011).
- [8] D. F. Wilson, W. M. Lee, S. Makonnen, O. Finikova, S. Apreleva, and S. A. Vinogradov, *J. Appl. Physiol.* **101**, 1648–1656 (2006).
- [9] E. G. Mik, C. Donkersloot, N. J. Raat, and C. Ince, *Photochem. Photobiol.* **76**, 12–21 (2002).
- [10] E. G. Mik, J. Stap, M. Sinaasappel, J. F. Beek, J. A. Aten, T. G. van Leeuwen, and C. Ince, *Nat. Methods* **3**, 939–945 (2006).
- [11] L. C. Gardner, S. J. Smith, and T. M. Cox, *J. Biol. Chem.* **266**, 22010–22018 (1991).
- [12] E. G. Mik, T. Johannes, C. J. Zuurbier, A. Heinen, J. H. Houben-Weerts, G. M. Balestra, J. Stap, J. F. Beek, and C. Ince, *Biophys. J.* **95**, 3977–3990 (2008).
- [13] E. G. Mik, C. Ince, O. Eerbeek, A. Heinen, J. Stap, B. Hooibrink, C. A. Schumacher, G. M. Balestra, T. Johannes, J. F. Beek, A. F. Nieuwenhuis, P. van Horsen, J. A. Spaan, and C. J. Zuurbier, *J. Mol. Cell Cardiol.* **46**, 943–951 (2009).
- [14] J. Morgan and A. R. Oseroff, *Adv. Drug Deliv. Rev.* **49**, 71–86 (2001).
- [15] H. Fukuda, A. Casas, and A. Battle, *Int. J. Biochem. Cell Biol.* **37**, 272–276 (2005).
- [16] C. J. Kelty, N. J. Brown, M. W. Reed, and R. Ackroyd, *Photochem. Photobiol. Sci.* **1**, 158–168 (2002).



- [17] Q. Peng, T. Warloe, K. Berg, J. Moan, M. Kongshaug, K. E. Giercksky, and J. M. Nesland, *Cancer* **79**, 2282–2308 (1997).
- [18] T. L. Becker, A. D. Paquette, K. R. Keymel, B. W. Henderson, and U. Sunar, *Biomed. Opt. Express* **2**, 123–130 (2010).
- [19] A. Juzeniene, P. Juzenas, and J. Moan, *Methods Mol. Biol.* **635**, 97–106 (2010).
- [20] R. Bezemer, D. J. Faber, E. Almac, J. Kalkman, M. Legend, M. Heger, and C. Ince, *Med. Biol. Eng. Comput.* **48**, 1233–1242 (2010).
- [21] A. S. Golub, A. S. Popel, L. Zheng, and R. N. Pittman, *Biophys. J.* **73**, 452–465 (1997).
- [22] H. C. De Vrijlder, T. Middelburg, H. S. De Bruijn, H. A. Martino Neumann, H. C. Sterenborg, D. J. Robinson, and E. R. De Haas, *G. Ital. Dermatol. Venereol.* **144**, 433–439 (2009).
- [23] J. S. Orringer, D. L. Sachs, E. Bailey, S. Kang, T. Hamilton, and J. J. Voorhees, *J. Cosmet. Dermatol.* **9**, 28–34 (2010).
- [24] E. S. Schweiger, C. C. Riddle, and D. J. Aires, *J. Drugs Dermatol.* **10**, 381–386 (2011).
- [25] R. N. Manifold and C. D. Anderson, *Arch. Dermatol. Res.* **303**, 285–292 (2011).
- [26] F. M. Piffaretti, K. Santhakumar, E. Forte, H. E. van den Bergh, and G. A. Wagnieres, *J. Biomed. Opt.* **16**, 037005 (2011).
- [27] T. Johannes, E. G. Mik, and C. Ince, *J. Appl. Physiol.* **100**, 1301–1310 (2006).

+++ NEW +++ NEW +++ NEW +++ NEW +++ NEW +++ NEW +++ NEW +++



2011. 900 pages, 266 figures,  
35 in color, 28 tables.  
Hardcover.  
ISBN: 978-3-527-40956-3

GABRIEL CRISTOBAL, PETER SCHELKENS, and HUGO THIENPONT (eds.)

## Optical and Digital Image Processing

*Fundamentals and Applications*

In recent years, Moore's law has fostered the steady growth of the field of digital image processing, though the computational complexity remains a problem for most of the digital image processing applications. In parallel, the research domain of optical image processing has matured, potentially bypassing the problems digital approaches were suffering and bringing new applications. The advancement of technology calls for applications and knowledge at the intersection of both areas but there is a clear knowledge gap between the digital signal processing

and the optical processing communities. This book covers the fundamental basis of the optical and image processing techniques by integrating contributions from both optical and digital research communities to solve current application bottlenecks, and give rise to new applications and solutions. Besides focusing on joint research, it also aims at disseminating the knowledge existing in both domains. Applications covered include image restoration, medical imaging, surveillance, holography, etc...

Register now for the free  
**WILEY-VCH Newsletter!**  
[www.wiley-vch.de/home/pas](http://www.wiley-vch.de/home/pas)

WILEY-VCH • P.O. Box 10 11 61 • 69451 Weinheim, Germany  
Fax: +49 (0) 62 01 - 60 61 84  
e-mail: [service@wiley-vch.de](mailto:service@wiley-vch.de) • <http://www.wiley-vch.de>